Optical generation of tunable ultrasonic waves

Keith A. Nelson, R. J. Dwayne Miller, D. R. Lutz, and M. D. Fayer
Chemistry Department, Stanford University, Stanford, California 94305

(Received 4 September 1981; accepted for publication 6 October 1981)

A convenient method of optically exciting and monitoring coherent acoustic waves in transparent or light-absorbing liquids and solids is described. The acoustic frequency is easily and continuously tunable from ≈ 3 MHz to at least 30 GHz with our experimental apparatus and in principle over a considerably wider range. In anisotropic materials any propagation direction can be selected. The optically generated acoustic waves can be optically amplified, cancelled, or phase shifted.

PACS numbers: 78.20.Hp, 43.35.Bf, 43.35.Cg

I. INTRODUCTION

Optical generation of ultrasonic waves has been of interest to workers in nonlinear optics, acoustics, and condensed matter spectroscopy for some time.[1,2] The interaction between light and material acoustic fields is of interest in its own right; furthermore, efficient light to ultrasound conversion holds promise for a variety of scientific and practical applications.

In this paper we describe a convenient method for optical excitation of coherent acoustic waves in transparent or light-absorbing liquids and solids. The acoustic frequency can be continuously and easily varied from about 3 MHz to 30 GHz with our experimental apparatus, and a considerably wider range should be possible. Once generated, the ultrasonic waves can be optically cancelled (turned off), amplified, or phase shifted. In anisotropic media (crystals, liquid crystals, stretched films, etc.) any propagation direction can be selected.

The technique, called Laser Induced Phonons (LIPS), is illustrated schematically in Fig. 1 and works as follows. Two ~ 100-psec, time-coincident laser pulses intersect inside the sample, setting up an optical interference pattern, i.e., alternating intensity peaks and nulls. Energy deposited into the system via optical absorption or stimulated Brillouin scattering results in the launching of counterpropagating ultrasonic waves (phonons) whose wavelength and orientation match the interference pattern geometry. The acoustic wavelength d is given by

$$d = \frac{\lambda}{2\sin(\theta/2)}, \tag{1}$$

where λ is the wavelength of the excitation pulses and θ is the angle between them (see Fig. 1). With the laser system in our laboratory we can vary d between about 1 mm and 0.1 μm, i.e., over a range of four orders of magnitude. In most materials this corresponds to tunable acoustic frequencies from about 3 MHz to 30 GHz.

The acoustic wave propagation, which continues long after the excitation pulses leave the sample, causes time-dependent, spatially periodic variations in the material density, and since the sample's optical properties (real and imaginary parts of the index of refraction) are density-dependent, the irradiated region of the sample acts as a Bragg diffraction grating. This propagation of the optically excited ultrasonic waves can be optically monitored by time-dependent Bragg diffraction of a variably delayed probe laser pulse.

The mechanism by which LIPS ultrasonic waves are generated depends upon whether the sample is optically absorbing or transparent at the excitation wavelength. If the excitation pulses are absorbed into high-lying vibronic levels, rapid radiationless relaxation and local heating at the interference maxima (the transient grating peaks) occurs. Thermal expansion then drives material in phase away from the grating peaks and toward the grating nulls, setting up counterpropagating waves. The acoustic response to absorbed excitation pulses, in terms of relative material displacement (strain), has been shown to be[3,4]

$$\begin{aligned} S_{yy} &= A\{\cos ky - \tfrac{1}{2}[\cos(\omega t + ky) + \cos(\omega t - ky)]\} \\ &= A\cos ky(1 - \cos \omega t), \end{aligned} \tag{2}$$

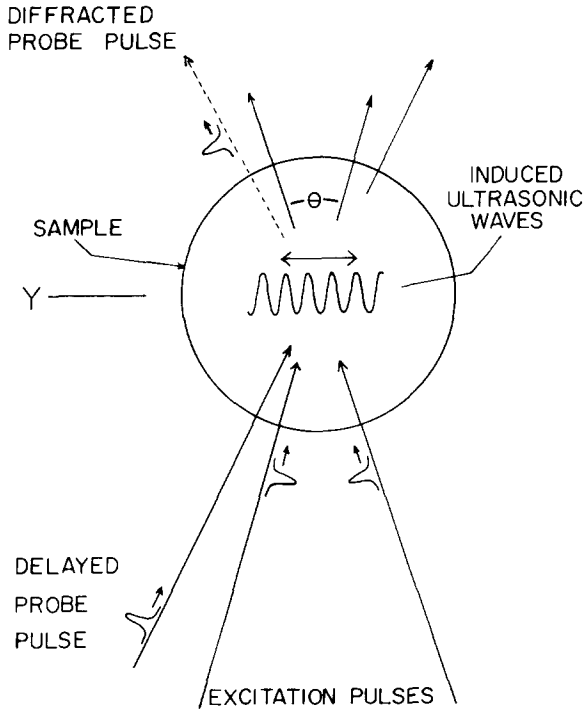

FIG. 1. Schematic illustration of the LIPS transient grating experiment. The crossed excitation pulses generate counterpropagating acoustic waves (phonons) with the wavelength and orientation of the optical interference pattern. Phonon-induced changes in the real or imaginary part of the index of refraction create a diffraction grating which Bragg diffracts the delayed probe pulse. The phonon wavelength is given by $d = \lambda/2\sin(\theta/2)$, where λ is the excitation wavelength and θ is the angle between the beams. The phonon frequency is continuously tunable by varying θ.

 0021-8979/82/021144-06$02.40

where S_{yy} is the compressional strain along the y-direction, A is the amplitude of the acoustic disturbance, k is the grating (phonon) wave vector, and ω is the acoustic frequency. ($\omega/k = v_y$, the longitudinal speed of sound along the y-direction in the medium.) The excitation geometry is as shown in Fig. 1. The acoustic disturbance in Eq. (2) can be viewed as a steady-state expansion (the dc term) plus a transient response (the counterpropagating waves). For simplicity we assume propagation of a single, longitudinal wave, although we have demonstrated and will illustrate below that in anisotropic media quasilongitudinal and quasitransverse waves can also be generated.[3] Local changes in material density ρ are given by

$$\delta\rho = -\rho_0 S_{yy}, \tag{3}$$

where ρ_0 is the normal density.

The excitation pulses are taken to be instantaneous and cross inside the sample at $t = 0$. At this time $\delta\rho = 0$ everywhere, i.e., the density is uniform. Material then moves away from the peaks and toward the nulls, causing the density at the peaks to decrease and the density at the nulls to increase. The density excursion is largest at $t = \pi/\omega$ (and $t = 3\pi/\omega$, $5\pi/\omega$, etc.), and returns to normal at $t = 2\pi/\omega$, $4\pi/\omega$, etc. (after each acoustic cycle). Thus the density at the grating peaks oscillates between normal and a reduced value, while the density at the grating nulls oscillates between normal and an increased value. The variably delayed probe pulse undergoes no diffraction at $t = 0, 2\pi/\omega$, etc. (uniform density), and is most strongly diffracted at $t = \pi/\omega, 3\pi/\omega$, etc. (maximum density excursion).

In samples which are transparent at the excitation wavelength, optical energy is coupled directly into the sample's acoustic field via stimulated Brillouin scattering.[4] This process takes advantage of the inherent spectral linewidth in the 100-ps excitation pulses. Higher-frequency photons from each pulse are annihilated to create lower-frequency photons in the opposite pulse and phonons of the difference frequency and wave vector in the medium. Counterpropagating waves (a standing wave) are thus produced. The acoustic response has been predicted earlier to be[4]

$$\begin{aligned} S_{yy} &= (-B/2)[\sin(\omega t + ky) + \sin(\omega t - ky)] \\ &= -B\cos ky \sin \omega t, \end{aligned} \tag{4}$$

where B is the acoustic wave amplitude. Experimental observations of this acoustic response are presented below. Notice that since there is no radiationless relaxation or heating, no static thermal expansion occurs. [Compare with Eq. (2).] The density at any point in the sample oscillates both above and below normal, and the density is normal everywhere ($\delta\rho \equiv 0$) at $t = 0, \pi/\omega, 2\pi/\omega$, etc. (*twice* each acoustic cycle). Thus the variably delayed probe pulse undergoes no diffraction twice each acoustic cycle. The different time-dependences of the diffracted signal arising from the two acoustic wave generating mechanisms allows simple determination of the mechanism of phonon excitation in a LIPS experiment.

In the next section, our experimental setup is described. In Sec. III, experimental results illustrating the two mechanisms of acoustic wave generation are presented. Additional data is shown which demonstrates that the optically excited ultrasonic waves can be optically manipulated (amplified, cancelled, or phase shifted). An illustration of LIPS effects in anisotropic media is also presented. In Sec. IV, applications of the LIPS effect are discussed.

II. EXPERIMENTAL

The LIPS experimental setup is illustrated in Fig. 2. The laser is a continuously pumped Nd:YAG system which is acousto-optically mode locked and Q-switched to produce high repetition rate (400 Hz), high-power infrared (1.06-μm)

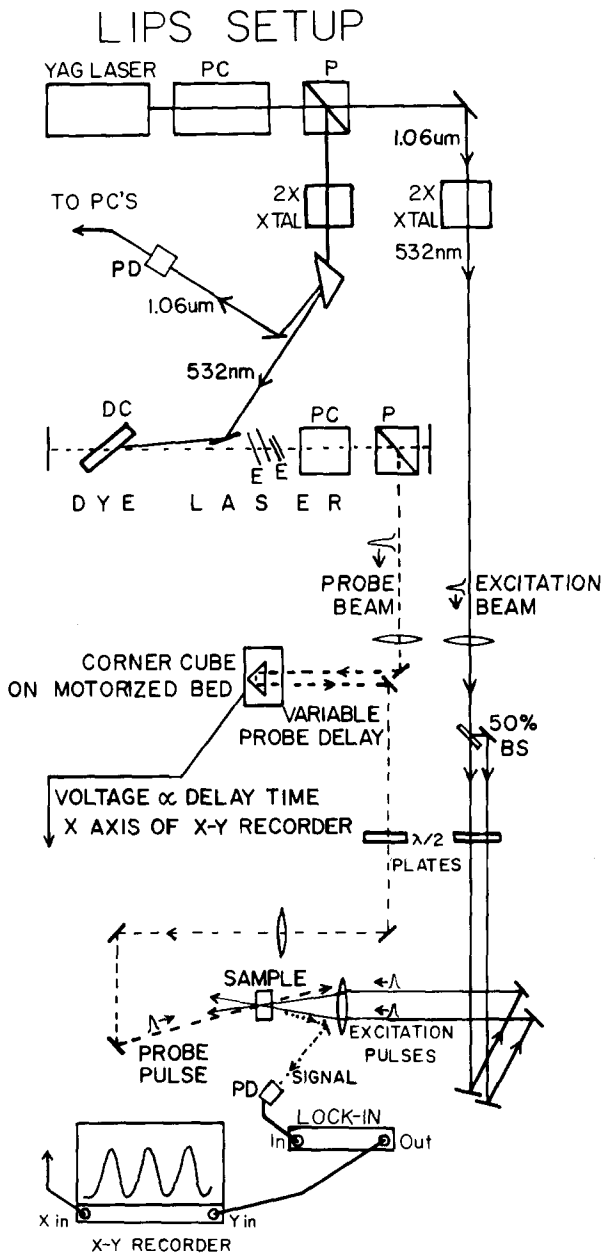

FIG. 2. Transient grating experimental setup. A single 1.06-μm pulse is selected from the Nd:YAG mode-locked pulse train and frequency doubled to 532 nm, then split into the two excitation pulses and recombined at the sample to generate the counterpropagating waves and transient grating. The rest of the pulse train is frequency doubled to synchronously pump a tunable dye laser whose output probes the grating after a variable delay. The Bragg-diffracted part of the probe pulse is the transient grating signal. PC≡Pockels cell; P≡polarizer; PD≡photodiode; DC≡dye cell; E≡etalon; BS≡beamsplitter.

subnanosecond pulses. The laser output is a train of about 40 mode-locked pulses, 5.7 ns apart, with ~ 1.4 mJ total energy. A large pulse from the train is selected by a Pockels cell with avalanche transistor driver. (In some experiments the Pockels cell window was widened to select two pulses, 5.7 ns apart.) The single pulse is frequency doubled using CD*A to give a 10-μJ, 80-ps, transform limited, TEM_{00} pulse at 532 nm. This passes through a 50% beamsplitter to create the two excitation pulses, which travel equal distances and are focused into the sample.

The unused infrared pulse train comes off a reflecting polarizer into another CD*A doubler crystal, and the 532-nm light is used to synchronously pump a dye laser which is spectrally narrowed and tuned by two intracavity etalons. The dye laser is cavity dumped using another Pockels cell with avalanche transistor driver to give a 6-μJ, 30-ps pulse with a spectral width of ~ 1 cm^{-1}. Synchronization of the two Pockels cells is obtained by a single avalanche transistor which itself is triggered by the infrared pulse train. The dye laser output travels a variable distance controlled by a motorized delay line consisting of a corner cube drawn along a precision optical rail. It probes the grating at an angle satisfying the Bragg diffraction condition. Excitation and probe spot sizes were 150 and 100 μm, respectively.

The diffracted probe intensity was measured with a p-i-n photodiode and lock-in amplifier which drives the y-axis of an x-y recorder. The x-axis is driven by a variable voltage derived from a 10-turn potentiometer connected to the delay line motor, providing the time scale. When the delay line is run, the time-dependent diffracted signal is recorded directly on the x-y recorder. In the experiments described below, the samples were solutions of cresyl violet perchlorate (Eastman) in ethanol (2.7×10^{-3} M) and malachite green (Eastman) in ethanol (concentrations given below). The solutions were mounted in a rotating dye cell to avoid heating effects. In the experiments on pure ethanol and low concentration malachite green in ethanol (presented in Fig. 3), the solutions were mounted in a 1-cm cuvette. The results obtained were independent of the laser repetition rate, indicating that residual heating effects from shot to shot were not present.

III. RESULTS AND DISCUSSION

Figure 3 shows LIPS data from pure ethanol and from solutions of malachite green in ethanol. The 532-nm excitation light is absorbed by malachite green but not by ethanol. The grating fringe spacing is 2.47 μm and the speed of sound in ethanol is 1.16×10^5 cm/sec.[5] The acoustic frequency is therefore $\omega = 2.95\times 10^9$ s^{-1}, and the acoustic period $\tau_{ac} = 2.13$ ns. (The acoustic period is the time required for ultrasonic waves to travel one fringe spacing.) Figure 3(a) shows LIPS data from pure ethanol. The important feature is the frequency of oscillations in the diffracted intensity. Signal vanishes every 1.07 ns, or exactly twice each acoustic cycle. This indicates that the acoustic disturbance is as given in Eq. (4), and that stimulated Brillouin scattering is responsible for acoustic wave production. This is to be expected since the green excitation light is not absorbed by pure ethanol.

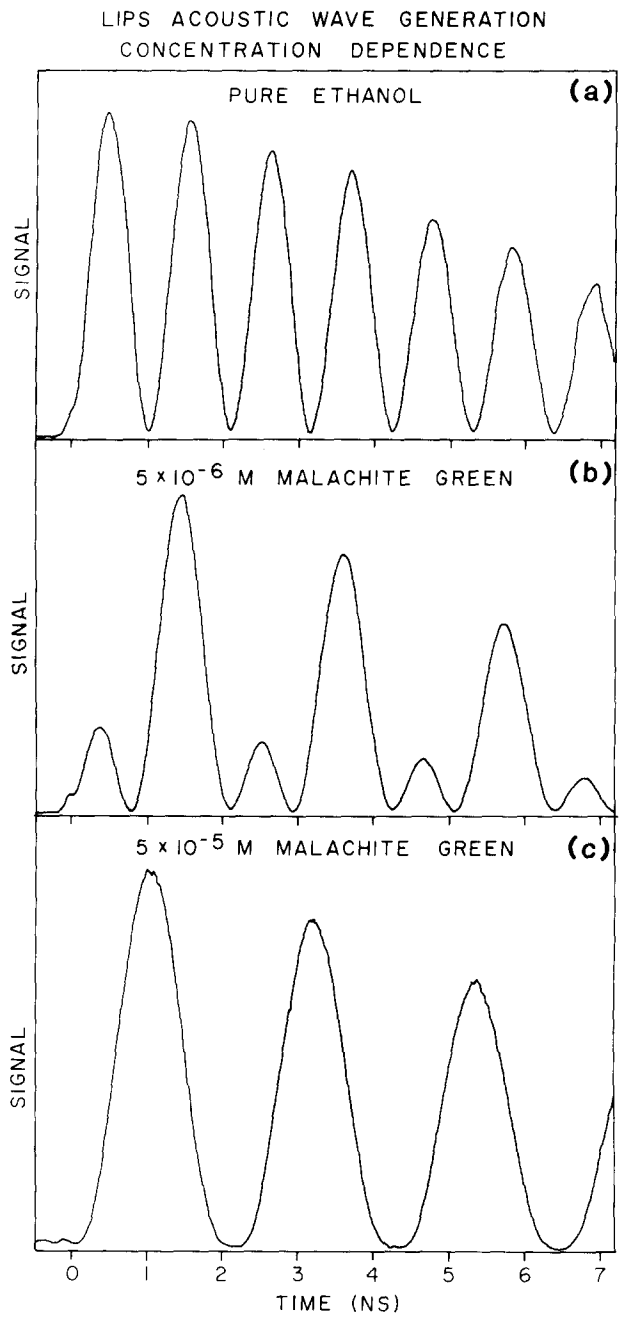

FIG. 3. LIPS transient grating data from pure ethanol and solutions of malachite green in ethanol. Excitation $\lambda = 532$ nm; probe $\lambda = 566$ nm. Fringe spacing $d = 2.47$ μm; acoustic cycle $\tau_{ac} = 2.13$ ns. Experimental conditions other than sample were identical throughout. (a) Pure ethanol. Electrostrictively-generated standing wave causes diffraction intensity to oscillate twice each acoustic cycle. (b) 5×10^{-6} M malachite green in ethanol. Electrostriction and optical absorption produce comparable responses. (c) 5×10^{-5} M malachite green in ethanol. Optical absorption effects dominate. Diffracted signal oscillates once each acoustic cycle.

Figure 3(c) shows data from a solution for 5×10^{-5} M malachite green in ethanol. This concentration is such that the acoustic disturbance due to optical absorption completely obscures that due to electrostriction. The diffracted intensity vanishes once each acoustic cycle, indicating that the acoustic response is as given in Eq. (2). Figure 3(b) shows data from a solution of intermediate malachite green concentration. Optical absorption and electrostriction excite acoustic responses of comparable magnitudes, and the effects of both

mechanisms are observed. The total acoustic disturbance is simply the sum of Eqs. (2) and (4) with appropriately weighted amplitudes A and B. Diffracted signal at any time goes as the square of the density excursion inside the material, calculated from Eq. (3). Equations (1)–(4) predict the positions and relative amplitudes of the signal maxima for any concentration of absorbing species, and a gradual transition from data of the form in Fig. 3(a) to that in Fig. 3(c) is predicted and was observed for a large number of intermediate concentration solutions. The amplitude of the acoustic response to optically absorbed excitation pulses ["A" in Eq. (2)] has been quantitatively related to the absorption strength and to thermal expansion and elastic stiffness coefficients of the sample.[3] The amplitude of the electrostrictively generated waves ["B" in Eq. (4)] has been similarly related to the sample's electrostrictive (photoelastic) constants.[4] Comparison of the acoustic response due to a known amount of absorption to the electrostrictively generated response, using data such as that in Fig. 3(b), will permit accurate measurements of photoelastic constants to be made.

It is of interest to note that only very weak absorption is needed to produce a detectable "heating" acoustic response. For example, with Nd:YAG fundamental (1.06-μm) excitation pulses, absorption into vibrational overtones of water produces a response which obscures the electrostrictively generated response. With deuterated water (or with H_2O and 532-nm excitation), electrostriction effects dominate. Similar results have been obtained with benzene and deuterated benzene. These results will be discussed in detail in a subsequent publication.[6] By tuning the excitation wavelength, an overtone absorption spectrum could be taken. The absorption strenghts could be determined by measurement of the absolute diffraction efficiency, or by comparison to the diffraction from a standard solution with a known amount of absorption. This is essentially a form of optoacoustic spectroscopy, highly sensitized by the concentration of acoustic energy into a single acoustic mode.

We now present experimental results which show that the optically generated LIPS ultrasonic waves can be optically manipulated (amplified, cancelled, or phase shifted). Figure 4(a) shows LIPS data from a solution of cresyl violet in ethanol. The grating fringe spacing is $d = 1.70\,\mu$m and the acoustic frequency $\omega = 4.26\times10^9\,\mathrm{s}^{-1}$. The excitation pulses are absorbed by cresyl violet, and the data shows one oscillation per acoustic cycle ($\tau_{ac} = 1.48$ ns). Ultrasonic wave propagation continues undisturbed until $t = 5.71$ ns, at which time a second pair of excitation pulses passes through the sample. [See inset Fig. 4(a).] Thereafter the effects of both pairs of excitation pulses are observed. It is clear that the second set of excitation pulses has amplified the acoustic disturbance.

From Eq. (2), the acoustic repsonse to two pairs of absorbed excitation pulses of equal magnitude and separated by a time t' is

$$S_{yy} = A\cos ky[2 - \cos\omega t - \cos(\omega t - \omega t')]$$
$$= 2A\cos ky[1 - \cos(\omega t'/2)\cos(\omega t - \omega t'/2)], \quad (5)$$

for $t > t'$. As before, the initial pair of excitation pulses passes through the sample at $t = 0$. Note that for a second pair of

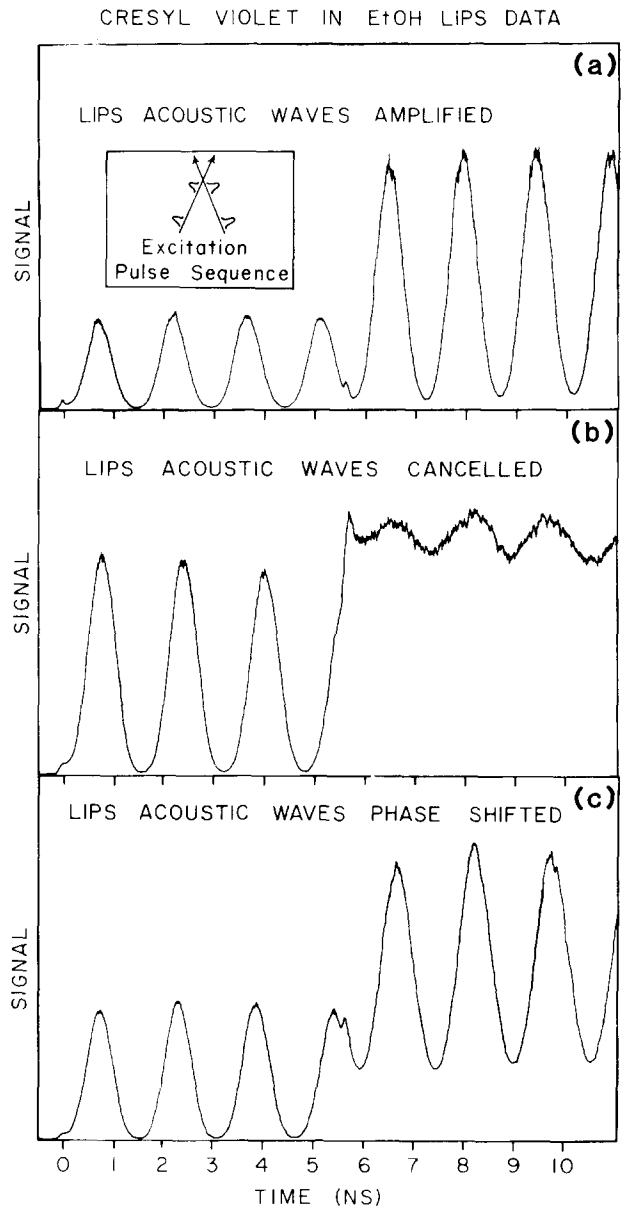

FIG. 4. LIPS results for a 2.7×10^{-3} M cresyl violet in ethanol solution. Excitation wavelength is 532.0 nm and probe wavelength is 597.1 nm in all cases. (a) Grating period $d = 1.70\,\mu$m and the acoustic frequency $\omega = 4.26\times10^9\,\mathrm{s}^{-1}$. A second pair of excitation pulses (see inset) impinges on the sample at $t' = 5.71\text{ ns} \approx 8\pi/\omega$ (in phase with counterpropagating waves). Acoustic disturbance is amplified. (b) Same as (a) except $d = 1.87$ μm, $\omega = 3.88\times10^9\,\mathrm{s}^{-1}$, and $t' = 5.71\text{ ns} = 7\pi/\omega$ (out of phase). Static acoustic response is amplified; counterpropagating waves are cancelled (turned off). (c) Same as (b) except $d = 1.79\,\mu$m, $\omega = 4.04\times10^9\,\mathrm{s}^{-1}$, and $t' = 5.71\text{ ns} = 7.34\,\pi/\omega$. Static acoustic response is amplified; counterpropagating waves are phase shifted.

pulses impinging on the sample at $t' = 0, 2\pi/\omega, 4\pi/\omega$, etc., the entire acoustic disturbance is amplified by a factor of two. (If the pairs of excitation pulses are of unequal magnitude, amplification by a different amount will occur.) In this case, the second pair of excitation pulses is in phase with the acoustic waves generated by the first pair. This is as in the experiment displayed in Fig. 4(a), where $t' = 5.7\text{ ns} \approx 8\pi/\omega$.

If $t' = \pi/\omega, 3\pi/\omega$, etc., the time-dependent part of Eq. (5) (i.e., the counterpropagating waves in the sample) will be cancelled when the second pair of excitation pulses passes

through the sample. The static density variation is amplified in either case, as shown by the time-independent part of Eq. (5). Figure 4(b) shows data taken under identical conditions as that in Fig. 4(a) except that the angle between the excitation pulses was changed to make the grating period $d = 1.87$ μm and the acoustic frequency $\omega = 3.88 \times 10^9\ s^{-1}$. Thus $t' = 5.7$ ns $= 7\pi/\omega$, and the counterpropagating waves are essentially cancelled (turned off) by the second set of pulses. The increased time-independent diffraction at $t > t'$ is due to the amplified, static density response.

Inspection of Eq. (5) shows that, in general, the counterpropagating waves are phase shifted by an amount $(\omega t'/2)$ and their amplitude is modified by a factor of $\cos(\omega t'/2)$. Thus the waves can be amplified, cancelled, or phase shifted. Figure 4(c) shows data taken with the grating period $d = 1.79$ μm, $\omega = 4.04 \times 10^9\ s^{-1}$, and $t' = 5.7$ ns $= 7.34$ π/ω. Thus the counterpropagating waves are phase shifted 60° forward.

The data in Fig. 4 allow direct visualization for the static density responses, providing further verification that Eq. (2) correctly describes the acoustic disturbance due to a single pair of absorbed excitation pulses. They also illustrate the extent to which the acoustic waves, once generated, can be optically manipulated. With many successive pairs of excitation pulses, repeated amplifications, on-off sequences, or phase shifts could take place. In the case of electrostrictively generated waves, the same manipulations would be possible with no residual signal due to the static density variation.

It is also interesting to consider the effects of optically phase shifting one of the second pair of excitation pulses or physically translating a second pair of exictation pulses such that their interference maxima coincided with the original interference minima, and vice versa. Either approach would cancel the *static* density variation, and amplify, cancel, or phase shift the counterpropagating waves, depending on the timing. Thus both the static and time-dependent acoustic responses can be optically manipulated.

Finally, we wish to illustrate the results of LIPS ultrasonic wave generation in anisotropic media. Figure 5 shows LIPS data from the monoclinic molecular crystal α-perylene. This has been discussed in detail earlier.[3,7] Excitation and probe wavelengths were 532 nm and were weakly absorbed by the sample, leading to one oscillation per acoustic cycle. In Figs. 5(a) and 5(b), the grating was aligned along the **b** and **a** crystallographic axes, respectively, and single longitudinal waves were generated. With the grating aligned between the $\bar{a}$ and $\bar{b}$ axes in the $\bar{a}$ $\bar{b}$ plane, quasilongitudinal and quasitransverse waves of different frequencies were generated. The theory of LIPS acoustic wave generation in anisotropic media has been detailed earlier,[3] and predicts the observed results. In anisotropic media, pure longitudinal waves or quasilongitudinal and quasitransverse waves will be generated depending upon grating orientation. Anisotropic acoustic parameters (velocities and attenuations) can thus be measured with this technique.[3]

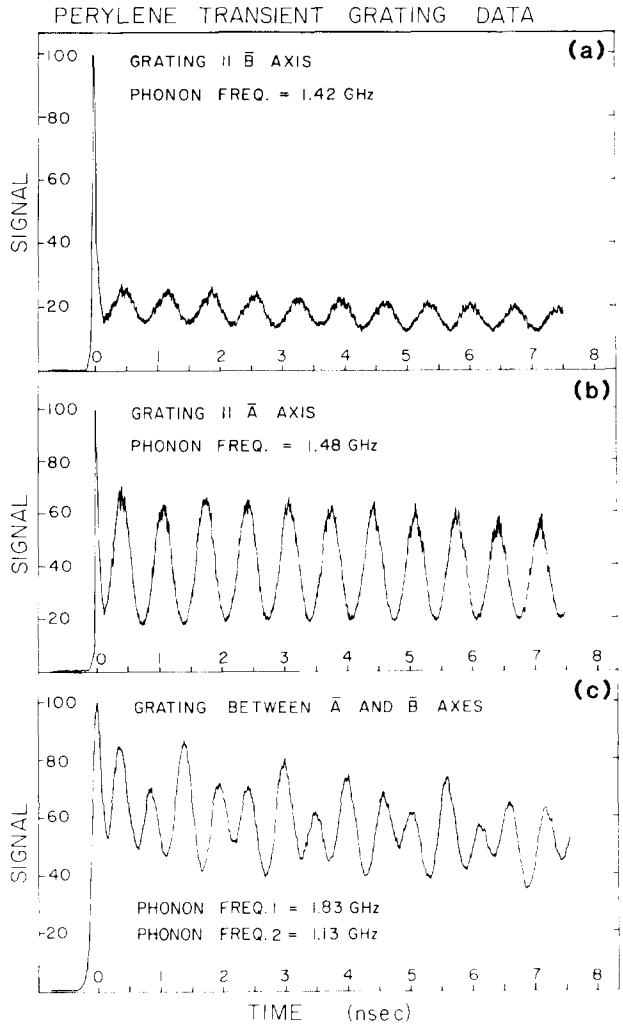

FIG. 5. LIPS results for pure α-perylene single crystals. Acoustic wavelength is 1.73 μm in all cases. The narrow spikes at $t = 0$ have no bearing on the subsequent data. (See Ref. 7.) (a) Acoustic waves propagate along the $\bar{b}$ (symmetry) axis. Single-frequency modulation is observed (longitudinal wave). (b) Acoustic waves propagate along the $\bar{a}$ axis; single-frequency modulation is observed (longitudinal wave). (c) Waves propagate between $\bar{a}$ and $\bar{b}$ axes, in $\bar{a}$ $\bar{b}$ plane. Beating is due to generation of quasilongitudinal and quasitransverse waves of identical wavelength but having different frequencies (dispersions).

IV. CONCLUDING REMARKS

The LIPS technique is an extremely versatile tool for controlled optical generation of ultrasonic waves in condensed media. LIPS experiments have been performed on transparent and absorbing solutions, organic and inorganic crystals, glasses, and plastics. The effects have been observed from liquid helium temperatures to room temperature. Acoustic waves have been generated by stimulated Brillouin scattering and by optical absorption. With a mode-locked Nd:YAG system, the acoustic frequency can be varied between about 3 MHz and 30 GHz, and above 60 GHz in some materials. Any propagation direction can be selected, and in anisotropic materials quasilongitudinal and quasitransverse waves can be generated. Finally, we have demonstrated that the optically generated acoustic waves can be optically amplified, cancelled, or phase shifted.

A wide variety of applications for the LIPS effect should be possible. It has already been used to measure anisotropic elastic constants and density-dependent spectral shifts.[3,4] Acoustic attenuation could be measured by monitoring the traveling waves after they leave the excitation re-

gion. The probe pulse would strike the sample at a variable distance from the excitation region, and diffracted intensity as a function of distance would yield the attenuation parameter. After the traveling waves leave the excitation region (or after they have been cancelled), only the "static" acoustic response arising from the absorbing mechanism remains. Actually this decays slowly due to thermal diffusion, and measurement of its decay in crystals as a function of orientation yields the thermal diffusion tensors.[8] LIPS could find possible applications in the field of optical communications. The diffracted probe beam could be both amplitude and frequency (phase) modulated to carry information. The applicability of LIPS to measure photoelastic constants and absorption spectra of weakly absorbing materials has been described. Finally, nondestructive testing, acoustic microscopy, and acoustic holography should be facilitated with optically generated ultrasonic waves.

ACKNOWLEDGMENTS

R.J.D.M. would like to acknowledge the National Sciences and Engineering Research Council of Canada for a postgraduate scholarship. We would also like to thank the National Science Foundation (DMR 79-20380) for support of this research.

[1]C. F. Quate, C. D. W. Wilkinson, and D. K. Winslow, Proc. IEEE **53**, 1604 (1965); Norman M. Kroll, J. Appl. Phys. **36**, 34 (1965); G. Cachier, J. Acoust. Soc. Am. **49**, 974 (1971); K. H. Yang, P. L. Richards, and Y. R. Shen, J. Appl. Phys. **44**, 1417 (1973); W. Grill and D. Weis, Phys. Rev. Lett. **35**, 588 (1975); R. S. Meltzer and J. E. Rives, Phys. Rev. Lett. **38**, 421 (1977).

[2]H. Eichler and H. Stahl, J. Appl. Phys. **44**, 3429 (1973), and references therein.

[3]Keith A. Nelson and M. D. Fayer, J. Chem. Phys. **72**, 5202 (1980).

[4]Keith A. Nelson, D. R. Lutz, Larry Madison, and M. D. Fayer, Phys. Rev. B, **6**, 3261 (1981).

[5]K. Altenburg, Z. Phys. Chem. (Leipzig) **250**, 399 (1972).

[6]Keith A. Nelson, R. J. Dwayne Miller, R. Casalegno, and M. D. Fayer (unpublished).

[7]K. A. Nelson, D. D. Dlott, and M. D. Fayer, Chem. Phys. Lett. **64**, 88 (1979)

[8]H. Eichler, G. Salje, and H. Stahl, J. Appl. Phys. **44**, 5383 (1973); John R. Andrews and Robin M. Hochstrasser, Chem. Phys. Lett. **76**, 207 (1980).